Precise Study of the Z/γ^* Boson Transverse Momentum Distribution in $p\bar{p}$ Collisions Using a Novel Technique

V. M. Abazov,[35] B. Abbott,[73] M. Abolins,[62] B. S. Acharya,[29] M. Adams,[48] T. Adams,[46] G. D. Alexeev,[35] G. Alkhazov,[39] A. Alton,[61,*] G. Alverson,[60] G. A. Alves,[2] L. S. Ancu,[34] M. Aoki,[47] Y. Arnoud,[14] M. Arov,[57] A. Askew,[46] B. Åsman,[40] O. Atramentov,[65] C. Avila,[8] J. BackusMayes,[80] F. Badaud,[13] L. Bagby,[47] B. Baldin,[47] D. V. Bandurin,[46] S. Banerjee,[29] E. Barberis,[60] P. Baringer,[55] J. Barreto,[2] J. F. Bartlett,[47] U. Bassler,[18] V. Bazterra,[48] S. Beale,[6] A. Bean,[55] M. Begalli,[3] M. Begel,[71] C. Belanger-Champagne,[40] L. Bellantoni,[47] S. B. Beri,[27] G. Bernardi,[17] R. Bernhard,[22] I. Bertram,[41] M. Besançon,[18] R. Beuselinck,[42] V. A. Bezzubov,[38] P. C. Bhat,[47] V. Bhatnagar,[27] G. Blazey,[49] S. Blessing,[46] K. Bloom,[64] A. Boehnlein,[47] D. Boline,[70] T. A. Bolton,[56] E. E. Boos,[37] G. Borissov,[41] T. Bose,[59] A. Brandt,[76] O. Brandt,[23] R. Brock,[62] G. Brooijmans,[68] A. Bross,[47] D. Brown,[17] J. Brown,[17] X. B. Bu,[7] D. Buchholz,[50] M. Buehler,[79] V. Buescher,[24] V. Bunichev,[37] S. Burdin,[41,†] T. H. Burnett,[80] C. P. Buszello,[42] B. Calpas,[15] E. Camacho-Pérez,[32] M. A. Carrasco-Lizarraga,[32] B. C. K. Casey,[47] H. Castilla-Valdez,[32] S. Chakrabarti,[70] D. Chakraborty,[49] K. M. Chan,[53] A. Chandra,[78] G. Chen,[55] S. Chevalier-Théry,[18] D. K. Cho,[75] S. W. Cho,[31] S. Choi,[31] B. Choudhary,[28] T. Christoudias,[42] S. Cihangir,[47] D. Claes,[64] J. Clutter,[55] M. Cooke,[47] W. E. Cooper,[47] M. Corcoran,[78] F. Couderc,[18] M.-C. Cousinou,[15] A. Croc,[18] D. Cutts,[75] M. Ćwiok,[30] A. Das,[44] G. Davies,[42] K. De,[76] S. J. de Jong,[34] E. De La Cruz-Burelo,[32] F. Déliot,[18] M. Demarteau,[47] R. Demina,[69] D. Denisov,[47] S. P. Denisov,[38] S. Desai,[47] K. DeVaughan,[64] H. T. Diehl,[47] M. Diesburg,[47] A. Dominguez,[64] T. Dorland,[80] A. Dubey,[28] L. V. Dudko,[37] D. Duggan,[65] A. Duperrin,[15] S. Dutt,[27] A. Dyshkant,[49] M. Eads,[64] D. Edmunds,[62] J. Ellison,[45] V. D. Elvira,[47] Y. Enari,[17] S. Eno,[58] H. Evans,[51] A. Evdokimov,[71] V. N. Evdokimov,[38] G. Facini,[60] T. Ferbel,[58,69] F. Fiedler,[24] F. Filthaut,[34] W. Fisher,[62] H. E. Fisk,[47] M. Fortner,[49] H. Fox,[41] S. Fuess,[47] T. Gadfort,[71] A. Garcia-Bellido,[69] V. Gavrilov,[36] P. Gay,[13] W. Geist,[19] W. Geng,[15,62] D. Gerbaudo,[66] C. E. Gerber,[48] Y. Gershtein,[65] G. Ginther,[47,69] G. Golovanov,[35] A. Goussiou,[80] P. D. Grannis,[70] S. Greder,[19] H. Greenlee,[47] Z. D. Greenwood,[57] E. M. Gregores,[4] G. Grenier,[20] Ph. Gris,[13] J.-F. Grivaz,[16] A. Grohsjean,[18] S. Grünendahl,[47] M. W. Grünewald,[30] F. Guo,[70] J. Guo,[70] G. Gutierrez,[47] P. Gutierrez,[73] A. Haas,[68,‡] S. Hagopian,[46] J. Haley,[60] L. Han,[7] K. Harder,[43] A. Harel,[69] J. M. Hauptman,[54] J. Hays,[42] T. Head,[43] T. Hebbeker,[21] D. Hedin,[49] H. Hegab,[74] A. P. Heinson,[45] U. Heintz,[75] C. Hensel,[23] I. Heredia-De La Cruz,[32] K. Herner,[61] G. Hesketh,[60] M. D. Hildreth,[53] R. Hirosky,[79] T. Hoang,[46] J. D. Hobbs,[70] B. Hoeneisen,[12] M. Hohlfeld,[24] S. Hossain,[73] Z. Hubacek,[10] N. Huske,[17] V. Hynek,[10] I. Iashvili,[67] R. Illingworth,[47] A. S. Ito,[47] S. Jabeen,[75] M. Jaffré,[16] S. Jain,[67] D. Jamin,[15] R. Jesik,[42] K. Johns,[44] M. Johnson,[47] D. Johnston,[64] A. Jonckheere,[47] P. Jonsson,[42] J. Joshi,[27] A. Juste,[47,§] K. Kaadze,[56] E. Kajfasz,[15] D. Karmanov,[37] P. A. Kasper,[47] I. Katsanos,[64] R. Kehoe,[77] S. Kermiche,[15] N. Khalatyan,[47] A. Khanov,[74] A. Kharchilava,[67] Y. N. Kharzheev,[35] D. Khatidze,[75] M. H. Kirby,[50] J. M. Kohli,[27] A. V. Kozelov,[38] J. Kraus,[62] A. Kumar,[67] A. Kupco,[11] T. Kurča,[20] V. A. Kuzmin,[37] J. Kvita,[9] S. Lammers,[51] G. Landsberg,[75] P. Lebrun,[20] H. S. Lee,[31] S. W. Lee,[54] W. M. Lee,[47] J. Lellouch,[17] L. Li,[45] Q. Z. Li,[47] S. M. Lietti,[5] J. K. Lim,[31] D. Lincoln,[47] J. Linnemann,[62] V. V. Lipaev,[38] R. Lipton,[47] Y. Liu,[7] Z. Liu,[6] A. Lobodenko,[39] M. Lokajicek,[11] P. Love,[41] H. J. Lubatti,[80] R. Luna-Garcia,[32,‖] A. L. Lyon,[47] A. K. A. Maciel,[2] D. Mackin,[78] R. Madar,[18] R. Magaña-Villalba,[32] S. Malik,[64] V. L. Malyshev,[35] Y. Maravin,[56] J. Martínez-Ortega,[32] R. McCarthy,[70] C. L. McGivern,[55] M. M. Meijer,[34] A. Melnitchouk,[63] D. Menezes,[49] P. G. Mercadante,[4] M. Merkin,[37] A. Meyer,[21] J. Meyer,[23] N. K. Mondal,[29] G. S. Muanza,[15] M. Mulhearn,[79] E. Nagy,[15] M. Naimuddin,[28] M. Narain,[75] R. Nayyar,[28] H. A. Neal,[61] J. P. Negret,[8] P. Neustroev,[39] S. F. Novaes,[5] T. Nunnemann,[25] G. Obrant,[39] J. Orduna,[32] N. Osman,[42] J. Osta,[53] G. J. Otero y Garzón,[1] M. Owen,[43] M. Padilla,[45] M. Pangilinan,[75] N. Parashar,[52] V. Parihar,[75] S. K. Park,[31] J. Parsons,[68] R. Partridge,[75,‡] N. Parua,[51] A. Patwa,[71] B. Penning,[47] M. Perfilov,[37] K. Peters,[43] Y. Peters,[43] G. Petrillo,[69] P. Pétroff,[16] R. Piegaia,[1] J. Piper,[62] M.-A. Pleier,[71] P. L. M. Podesta-Lerma,[32,¶] V. M. Podstavkov,[47] M.-E. Pol,[2] P. Polozov,[36] A. V. Popov,[38] M. Prewitt,[78] D. Price,[51] S. Protopopescu,[71] J. Qian,[61] A. Quadt,[23] B. Quinn,[63] M. S. Rangel,[2] K. Ranjan,[28] P. N. Ratoff,[41] I. Razumov,[38] P. Renkel,[77] P. Rich,[43] M. Rijssenbeek,[70] I. Ripp-Baudot,[19] F. Rizatdinova,[74] M. Rominsky,[47] C. Royon,[18] P. Rubinov,[47] R. Ruchti,[53] G. Safronov,[36] G. Sajot,[14] A. Sánchez-Hernández,[32] M. P. Sanders,[25] B. Sanghi,[47] A. S. Santos,[5] G. Savage,[47] L. Sawyer,[57] T. Scanlon,[42] R. D. Schamberger,[70] Y. Scheglov,[39] H. Schellman,[50] T. Schliephake,[26] S. Schlobohm,[80] C. Schwanenberger,[43] R. Schwienhorst,[62] J. Sekaric,[55] H. Severini,[73] E. Shabalina,[23] V. Shary,[18] A. A. Shchukin,[38] R. K. Shivpuri,[28] V. Simak,[10] V. Sirotenko,[47] P. Skubic,[73] P. Slattery,[69] D. Smirnov,[53] K. J. Smith,[67] G. R. Snow,[64] J. Snow,[72] S. Snyder,[71] S. Söldner-Rembold,[43] L. Sonnenschein,[21] A. Sopczak,[41] M. Sosebee,[76] K. Soustruznik,[9] B. Spurlock,[76] J. Stark,[14] V. Stolin,[36] D. A. Stoyanova,[38] E. Strauss,[70] M. Strauss,[73] D. Strom,[48] L. Stutte,[47] P. Svoisky,[73] M. Takahashi,[43]

A. Tanasijczuk,[1] W. Taylor,[6] M. Titov,[18] V. V. Tokmenin,[35] D. Tsybychev,[70] B. Tuchming,[18] C. Tully,[66] P. M. Tuts,[68]
L. Uvarov,[39] S. Uvarov,[39] S. Uzunyan,[49] R. Van Kooten,[51] W. M. van Leeuwen,[33] N. Varelas,[48] E. W. Varnes,[44]
I. A. Vasilyev,[38] P. Verdier,[20] L. S. Vertogradov,[35] M. Verzocchi,[47] M. Vesterinen,[43] D. Vilanova,[18] P. Vint,[42] P. Vokac,[10]
H. D. Wahl,[46] M. H. L. S. Wang,[69] J. Warchol,[53] G. Watts,[80] M. Wayne,[53] M. Weber,[47,**] L. Welty-Rieger,[50]
M. Wetstein,[58] A. White,[76] D. Wicke,[24] M. R. J. Williams,[41] G. W. Wilson,[55] S. J. Wimpenny,[45] M. Wobisch,[57]
D. R. Wood,[60] T. R. Wyatt,[43] Y. Xie,[47] C. Xu,[61] S. Yacoob,[50] R. Yamada,[47] W.-C. Yang,[43] T. Yasuda,[47] Y. A. Yatsunenko,[35]
Z. Ye,[47] H. Yin,[7] K. Yip,[71] H. D. Yoo,[75] S. W. Youn,[47] J. Yu,[76] S. Zelitch,[79] T. Zhao,[80] B. Zhou,[61] J. Zhu,[61] M. Zielinski,[69]
D. Zieminska,[51] and L. Zivkovic[68]

(D0 Collaboration)

[1]*Universidad de Buenos Aires, Buenos Aires, Argentina*
[2]*LAFEX, Centro Brasileiro de Pesquisas Físicas, Rio de Janeiro, Brazil*
[3]*Universidade do Estado do Rio de Janeiro, Rio de Janeiro, Brazil*
[4]*Universidade Federal do ABC, Santo André, Brazil*
[5]*Instituto de Física Teórica, Universidade Estadual Paulista, São Paulo, Brazil*
[6]*Simon Fraser University, Vancouver, British Columbia, and York University, Toronto, Ontario, Canada*
[7]*University of Science and Technology of China, Hefei, People's Republic of China*
[8]*Universidad de los Andes, Bogotá, Colombia*
[9]*Charles University, Faculty of Mathematics and Physics, Center for Particle Physics, Prague, Czech Republic*
[10]*Czech Technical University in Prague, Prague, Czech Republic*
[11]*Center for Particle Physics, Institute of Physics, Academy of Sciences of the Czech Republic, Prague, Czech Republic*
[12]*Universidad San Francisco de Quito, Quito, Ecuador*
[13]*LPC, Université Blaise Pascal, CNRS/IN2P3, Clermont, France*
[14]*LPSC, Université Joseph Fourier Grenoble 1, CNRS/IN2P3, Institut National Polytechnique de Grenoble, Grenoble, France*
[15]*CPPM, Aix-Marseille Université, CNRS/IN2P3, Marseille, France*
[16]*LAL, Université Paris-Sud, CNRS/IN2P3, Orsay, France*
[17]*LPNHE, Universités Paris VI and VII, CNRS/IN2P3, Paris, France*
[18]*CEA, Irfu, SPP, Saclay, France*
[19]*IPHC, Université de Strasbourg, CNRS/IN2P3, Strasbourg, France*
[20]*IPNL, Université Lyon 1, CNRS/IN2P3, Villeurbanne, France and Université de Lyon, Lyon, France*
[21]*III. Physikalisches Institut A, RWTH Aachen University, Aachen, Germany*
[22]*Physikalisches Institut, Universität Freiburg, Freiburg, Germany*
[23]*II. Physikalisches Institut, Georg-August-Universität Göttingen, Göttingen, Germany*
[24]*Institut für Physik, Universität Mainz, Mainz, Germany*
[25]*Ludwig-Maximilians-Universität München, München, Germany*
[26]*Fachbereich Physik, Bergische Universität Wuppertal, Wuppertal, Germany*
[27]*Panjab University, Chandigarh, India*
[28]*Delhi University, Delhi, India*
[29]*Tata Institute of Fundamental Research, Mumbai, India*
[30]*University College Dublin, Dublin, Ireland*
[31]*Korea Detector Laboratory, Korea University, Seoul, Korea*
[32]*CINVESTAV, Mexico City, Mexico*
[33]*FOM-Institute NIKHEF and University of Amsterdam/NIKHEF, Amsterdam, The Netherlands*
[34]*Radboud University Nijmegen/NIKHEF, Nijmegen, The Netherlands*
[35]*Joint Institute for Nuclear Research, Dubna, Russia*
[36]*Institute for Theoretical and Experimental Physics, Moscow, Russia*
[37]*Moscow State University, Moscow, Russia*
[38]*Institute for High Energy Physics, Protvino, Russia*
[39]*Petersburg Nuclear Physics Institute, St. Petersburg, Russia*
[40]*Stockholm University, Stockholm and Uppsala University, Uppsala, Sweden*
[41]*Lancaster University, Lancaster LA1 4YB, United Kingdom*
[42]*Imperial College London, London SW7 2AZ, United Kingdom*
[43]*The University of Manchester, Manchester M13 9PL, United Kingdom*
[44]*University of Arizona, Tucson, Arizona 85721, USA*
[45]*University of California Riverside, Riverside, California 92521, USA*
[46]*Florida State University, Tallahassee, Florida 32306, USA*
[47]*Fermi National Accelerator Laboratory, Batavia, Illinois 60510, USA*
[48]*University of Illinois at Chicago, Chicago, Illinois 60607, USA*

[49]Northern Illinois University, DeKalb, Illinois 60115, USA
[50]Northwestern University, Evanston, Illinois 60208, USA
[51]Indiana University, Bloomington, Indiana 47405, USA
[52]Purdue University Calumet, Hammond, Indiana 46323, USA
[53]University of Notre Dame, Notre Dame, Indiana 46556, USA
[54]Iowa State University, Ames, Iowa 50011, USA
[55]University of Kansas, Lawrence, Kansas 66045, USA
[56]Kansas State University, Manhattan, Kansas 66506, USA
[57]Louisiana Tech University, Ruston, Louisiana 71272, USA
[58]University of Maryland, College Park, Maryland 20742, USA
[59]Boston University, Boston, Massachusetts 02215, USA
[60]Northeastern University, Boston, Massachusetts 02115, USA
[61]University of Michigan, Ann Arbor, Michigan 48109, USA
[62]Michigan State University, East Lansing, Michigan 48824, USA
[63]University of Mississippi, University, Mississippi 38677, USA
[64]University of Nebraska, Lincoln, Nebraska 68588, USA
[65]Rutgers University, Piscataway, New Jersey 08855, USA
[66]Princeton University, Princeton, New Jersey 08544, USA
[67]State University of New York, Buffalo, New York 14260, USA
[68]Columbia University, New York, New York 10027, USA
[69]University of Rochester, Rochester, New York 14627, USA
[70]State University of New York, Stony Brook, New York 11794, USA
[71]Brookhaven National Laboratory, Upton, New York 11973, USA
[72]Langston University, Langston, Oklahoma 73050, USA
[73]University of Oklahoma, Norman, Oklahoma 73019, USA
[74]Oklahoma State University, Stillwater, Oklahoma 74078, USA
[75]Brown University, Providence, Rhode Island 02912, USA
[76]University of Texas, Arlington, Texas 76019, USA
[77]Southern Methodist University, Dallas, Texas 75275, USA
[78]Rice University, Houston, Texas 77005, USA
[79]University of Virginia, Charlottesville, Virginia 22901, USA
[80]University of Washington, Seattle, Washington 98195, USA

Using 7.3 fb^{-1} of $p\bar{p}$ collisions collected by the D0 detector at the Fermilab Tevatron, we measure the distribution of the variable ϕ_η^*, which probes the same physical effects as the Z/γ^* boson transverse momentum, but is less susceptible to the effects of experimental resolution and efficiency. A QCD prediction is found to describe the general features of the ϕ_η^* distribution, but is unable to describe its detailed shape or dependence on boson rapidity. A prediction that includes a broadening of transverse momentum for small values of the parton momentum fraction is strongly disfavored.

Z/γ^* bosons are produced at hadron colliders via quark-antiquark annihilation. Their decays to e^+e^- and $\mu^+\mu^-$ can be detected with little background and the phenomenology is simplified by the absence of color flow between the incoming partons and the products of the boson decay, thus providing an excellent testing ground for QCD predictions. Z/γ^* bosons may be produced with a nonzero momentum in the plane transverse to the beam direction, $p_T^{\ell\ell}$, due to QCD radiation from the incoming partons. Resummation techniques [1] allow calculations of the distribution of $p_T^{\ell\ell}$ within the framework of perturbative QCD, even at relatively low $p_T^{\ell\ell}$ (e.g., $p_T^{\ell\ell} < 30$ GeV). However, additional nonperturbative form factors, such as that of BLNY [2], must be determined in global fits to experimental data. An increase of these form factors for $x < 10^{-2}$, where x is the parton momentum fraction, was

suggested [3] to improve the description of hadron production observed in deep inelastic electron-proton scattering at HERA. Since vector boson production corresponds typically to parton $x < 10^{-2}$ at the LHC, these modified form factors would lead to a broadening of the expected vector boson transverse momentum distributions [4]. This "small-x broadening" would influence the measurement of the W boson mass as well as searches for Higgs bosons and physics beyond the standard model at the LHC. It is important to study quantitatively such x dependencies at the Tevatron, where they can be probed using the dependence of the $p_T^{\ell\ell}$ distribution on boson rapidity, y [5]. At the Tevatron, bosons with $|y| > 2$ are particularly sensitive to the region $x < 10^{-2}$.

In the region of low $p_T^{\ell\ell}$, the precision of the most recent measurements at the Tevatron [6,7] was dominated by

uncertainties in correcting for experimental resolution and efficiency. Furthermore, the measurements were presented in a small number of relatively wide bins due the limited experimental resolution [8]. The variable a_T, which corresponds to the component of $p_T^{\ell\ell}$ that is transverse to the dilepton thrust axis, $\hat{t}$, has been proposed as an alternative analyzing variable that allows us to study the issues discussed above, but is less susceptible than the $p_T^{\ell\ell}$ to detector effects [9]. Figure 1 illustrates this and other relevant variables defined below. The a_T distribution was subsequently calculated to next-to-leading-log (NLL) accuracy using resummation techniques [10]. Additional analyzing variables with even better experimental resolution have recently been proposed and studied [11]. The optimal variable was found to be ϕ^*_η, which is defined as

$$\phi^*_\eta = \tan(\phi_{\mathrm{acop}}/2)\sin(\theta^*_\eta),$$

where ϕ_{acop} is the acoplanarity angle, given by $\phi_{\mathrm{acop}} = \pi - \Delta\phi^{\ell\ell}$, and $\Delta\phi^{\ell\ell}$ is the difference in azimuthal angle, ϕ, between the two lepton candidates. The variable θ^*_η is a measure of the scattering angle of the leptons with respect to the proton beam direction in the rest frame of the dilepton system. It is defined [11] by $\cos(\theta^*_\eta) = \tanh[(\eta^- - \eta^+)/2]$, where η^- and η^+ are the pseudorapidities [5] of the negatively and positively charged lepton, respectively.

The variable ϕ^*_η is highly correlated with the quantity $a_T/m_{\ell\ell}$, where $m_{\ell\ell}$ is the dilepton invariant mass. Since ϕ_{acop} and θ^*_η depend exclusively on the directions of the two leptons, which are measured with a precision of a milliradian or better, ϕ^*_η is experimentally very well measured compared to any quantities that rely on the momenta of the leptons.

We present a measurement of the normalized ϕ^*_η distribution, $(1/\sigma)(d\sigma/d\phi^*_\eta)$, in bins of $|y|$, using 7.3 fb^{-1} of $p\bar{p}$ collisions collected by the D0 detector at the Fermilab Tevatron. The ϕ^*_η distributions are measured in both dielectron and dimuon events and are corrected for experimental resolution and efficiency. When using Monte Carlo (MC) calculations to evaluate the correction factors, we apply the same kinematic selection criteria at the MC particle level as we apply in the selection of candidate

events in the data [12]. For this purpose, MC particle level electrons are defined as the four-vector sum of any electrons and photons within a cone of $\Delta\mathcal{R} = \sqrt{(\Delta\eta)^2 + (\Delta\phi)^2} < 0.2$ around an electron, where $\Delta\eta$ $(\Delta\phi)$ is the distance in η (ϕ) from the particle level electron; this mimics the measurement of electron energy in the calorimeter. MC particle level muons are defined after QED final state radiation; this mimics the measurement of muon momentum in the tracking detector. The kinematic selection criteria are: electrons must satisfy $p_T > 20$ GeV and $|\eta| < 1.1$ or $1.5 < |\eta| < 3$; muons must satisfy $p_T > 15$ GeV and $|\eta| < 2$; $m_{\ell\ell}$ must fall within the range 70–110 GeV.

The corrected data are compared to predictions from the MC program RESBOS [13] with the above kinematic selection criteria applied at the particle level. RESBOS generates Z/γ^* boson events with initial state QCD corrections to next-to-leading order (NLO) and NLL accuracy together with: the nonperturbative BLNY form factor [2], whose width is controlled primarily by the parameter g_2 (with default value $[0.68^{+0.02}_{-0.01}]$ GeV^2 [2]); an additional next-to-NLO (NNLO) K factor [14]; CTEQ6.6 NLO parton distribution functions (PDFs) [15]; and QED radiative corrections from PHOTOS [16]. The QCD factorization and renormalization scales are set event by event to the mass of the Z/γ^* boson propagator.

The D0 detector [17] consists of: silicon microstrip and central fiber tracking detectors, located within a 2 T superconducting solenoid; a liquid-argon/uranium sampling calorimeter; and an outer muon system consisting of tracking and scintillation detectors located before and after 1.8 T toroids. Candidate dielectron events are required to satisfy a trigger based on the identification of a single electron and to contain two clusters reconstructed in the calorimeter with a transverse and longitudinal shower profile consistent with that expected of an electron. The calorimeter is housed in three separate cryostats; this has the effect that electron identification is degraded in the region $1.1 < |\eta| < 1.5$. Candidate dimuon events are required to satisfy a trigger based on the identification of a single muon and to contain two muons reconstructed either in the outer muon system, or as an energy deposit consistent with the passage of a minimum-ionizing particle in the calorimeter. In order to ensure an accurate measurement of the lepton directions at the point of production, the two lepton candidates are required to be matched to a pair of oppositely charged particle tracks reconstructed in the central tracking detectors. Candidate leptons resulting from misidentified hadrons or produced by the decay of hadrons are suppressed by requiring that they be isolated from other particles in the event and, in the case of electrons with $|\eta| < 1.1$, by requiring the energy measured in the calorimeter and the momentum measured in the central tracking detectors to be consistent. Contamination from cosmic ray muons is strongly suppressed by a requirement
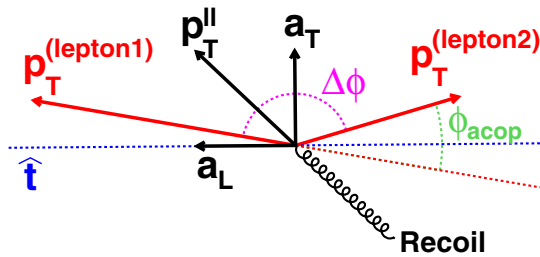

FIG. 1 (color online).   Illustration in the plane transverse to the beam direction of the variables defined in the text and used to analyze the dilepton transverse momentum.

that the muons originate from the $p\bar{p}$ collision point and by rejecting events in which the two muon candidates are back to back in η. In total, 455 k dielectron events and 511 k dimuon events are selected.

The corrections to the observed ϕ_η^* distribution for experimental resolution and efficiency are evaluated using Z/γ^* boson MC events that are generated with PYTHIA [18] and passed through a GEANT-based [19] simulation of the detector. These fully simulated MC events are reweighted at the generator level in two dimensions ($p_T^{\ell\ell}$ and $|y|$) to match the predictions of RESBOS. In addition, adjustments are made to improve the accuracy of the following aspects of the detector simulation: electron energy and muon p_T scale and resolution; track ϕ and η resolutions; trigger efficiencies; and relevant offline reconstruction and selection efficiencies. Variations in the above adjustments to the underlying physics and the detector simulation are included in the assessment of the systematic uncertainties on the correction factors.

The systematic uncertainties due to electron energy and muon p_T scale and resolution are small, and arise only due to the kinematic requirements in the event selection. The measured ϕ_η^* distribution is, however, susceptible to modulations in ϕ of the lepton identification and trigger efficiencies, which result, e.g., from detector module boundaries in the calorimeter and muon systems. Particular care has been taken (a) in the choice of lepton identification criteria in order to minimize such modulations and (b) to ensure that such modulations are well simulated in the MC calculations. For example, the requirements imposed on shower profile are much looser than those usually employed in electron identification within D0, because tight requirements are particularly inefficient in the regions close to module boundaries in the calorimeter. Similarly, the inclusion of muon

candidates identified in the calorimeter reduces the effect of gaps between modules in the outer muon system. Accurate modelling of the angular resolution of the central tracking detectors is another crucial aspect of this analysis. The resolution in ϕ and η is measured in the data using cosmic ray muons that traverse the detector, since these should produce events containing two tracks that are exactly back to back except for the effect of detector resolution.

Backgrounds from $Z \to \tau^-\tau^+$, $W \to \ell\nu$ (+ jets), and $WW \to \ell\nu\ell\nu$ are simulated using PYTHIA. Background from top quark pair events is simulated with ALPGEN [20], with PYTHIA used for parton showering. Background from multijet events is estimated from data. The total fraction of background events is 0.26% for the dielectron channel, and 0.38% for the dimuon channel.

Since the experimental resolution in ϕ_η^* is narrower than the chosen bin widths, the fractions of accepted events that fall within the same bin in ϕ_η^* at the particle level and reconstructed detector level in the MC calculations are high, having typical (lowest) values of around 98% (92%). Therefore, simple bin-by-bin corrections of the ϕ_η^* distribution are sufficient. In almost all ϕ_η^* bins the total systematic uncertainty is substantially smaller than the statistical uncertainty.

Figure 2 shows the corrected particle level ϕ_η^* distributions together with predictions from RESBOS. Figure 3 shows the ratio of the corrected ϕ_η^* distributions to the RESBOS predictions in both the dielectron and dimuon channels. The general shape of the distributions is broadly described by RESBOS over the full range in ϕ_η^*. However, the small statistical uncertainties resulting from the large dilepton data sets, combined with the fine binning and small systematic uncertainties resulting from the use of ϕ_η^* as the analyzing variable, reveal differences between
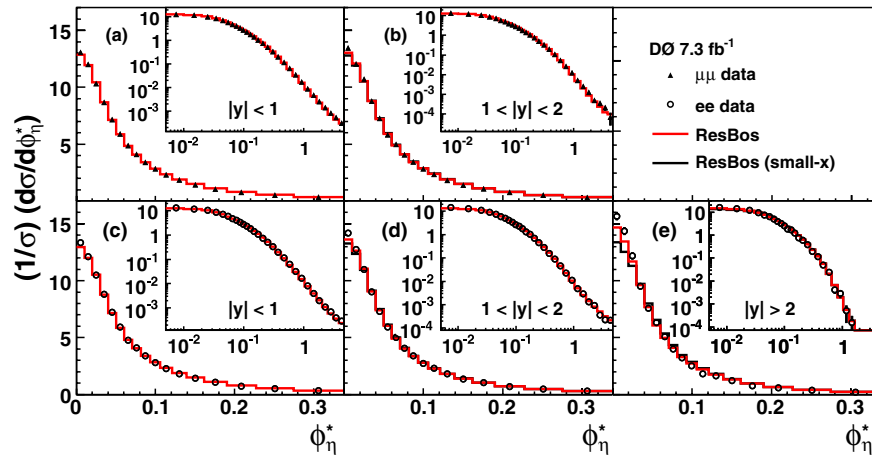

FIG. 2 (color online).   Corrected distributions of $(1/\sigma) \times (d\sigma/d\phi_\eta^*)$ for dimuon events with (a) $|y| < 1$ and (b) $1 < |y| < 2$; and dielectron events with (c) $|y| < 1$, (d) $1 < |y| < 2$ and (e) $|y| > 2$. The larger plots show the restricted range $0 < \phi_\eta^* < 0.34$ and the insets show the full range of ϕ_η^*. The predictions from RESBOS are shown as the red histogram and from RESBOS with small-x broadening as the black histogram [which is visible principally in (e)].
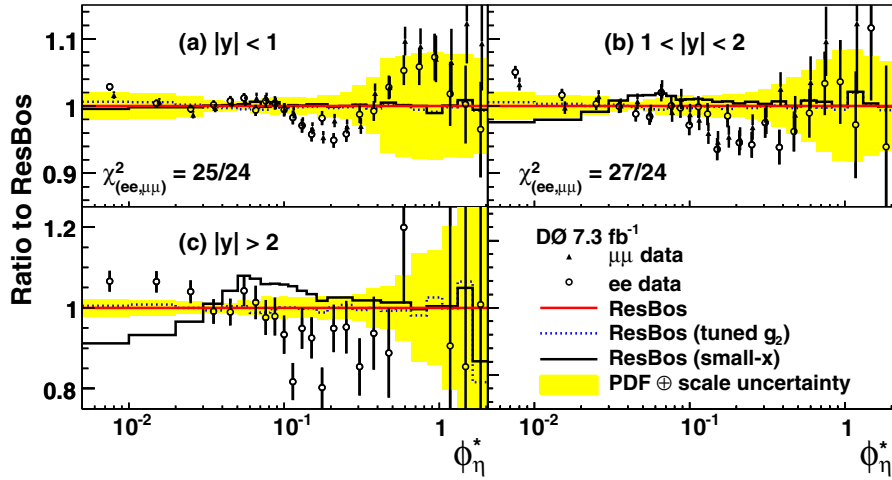
FIG. 3 (color online).   Ratio of the corrected distributions of $(1/\sigma) \times (d\sigma/d\phi_\eta^*)$ to RESBOS for: (a) $|y| < 1$, (b) $1 < |y| < 2$ and (c) $|y| > 2$. Statistical and systematic uncertainties are combined in quadrature. In (a) and (b) a χ^2 for the comparison of the dielectron and dimuon data, $\chi^2_{(ee/\mu\mu)}$, is calculated assuming uncorrelated uncertainties. The yellow band around the RESBOS prediction represents the quadrature sum of uncertainty due to PDFs (evaluated using the CTEQ6.6 NLO error PDFs [15]) and the uncertainty due to the QCD scale (evaluated by varying the factorization and renormalization scales simultaneously by a factor of 2). Also shown are the changes to the RESBOS predictions when g_2 is set to 0.66 GeV^2 (dotted blue line) and when the small-x broadening option is enabled (solid black line).

the data and RESBOS. Since the particle level definitions for electrons and muons to which the data are corrected are slightly different, Fig. 3 represents the most appropriate way to demonstrate the consistency of the dielectron and dimuon data. Given that the experimental corrections are very different in the two channels, this consistency represents a powerful cross check of the corrected distributions.

The results of fits for the value of g_2, separately in each $|y|$ bin and channel, are shown in Table I. It can be seen that the fitted values of g_2 show a monotonic decrease with increasing $|y|$ for both channels. That is, the width of the ϕ_η^* distribution becomes narrower with increasing $|y|$ faster in the data than is predicted by RESBOS. This is the opposite of the behavior expected from the small-x broadening hypothesis [3,4]. Figure 3 confirms that the prediction from RESBOS with small-x broadening is in poor agreement with data. It can also be seen that choosing the g_2 value (0.66 GeV^2) that best describes the average behavior of the data over all $|y|$ bins and channels has little effect on the level of agreement with data.

A previous measurement [7] showed that, for central rapidities, RESBOS underestimates the number of Z/γ^* bosons at high $p_T^{\ell\ell}$ by about 10%. This is consistent with the deviations seen at high values of ϕ_η^* in Fig. 3(a).

In summary, using 7.3 fb^{-1} of $p\bar{p}$ collisions collected by the D0 detector at the Fermilab Tevatron, we have studied with unprecedented precision the $p_T^{\ell\ell}$ distribution of Z/γ^* bosons in dielectron and dimuon final states. In bins of boson rapidity, the normalised cross section is measured as a function of the variable ϕ_η^*. Predictions from RESBOS are unable to describe the detailed shape of the corrected data, and a prediction that includes the effect of small-x broadening is strongly disfavored.

Tables of corrected $(1/\sigma)(d\sigma/d\phi_\eta^*)$ distributions for each $|y|$ bin and channel are provided [21].

TABLE I.   Value of g_2 (GeV^2) that best describes the corrected data in each $|y|$ bin and channel.

Channel	$|y| < 1$	$1 < |y| < 2$	$|y| > 2$
ee	0.644 ± 0.013	0.619 ± 0.017	0.550 ± 0.048
$\mu\mu$	0.670 ± 0.012	0.645 ± 0.019	-

*Visitor from Augustana College, Sioux Falls, SD, USA.
†Visitor from The University of Liverpool, Liverpool, United Kingdom.
‡Visitor from SLAC, Menlo Park, CA, USA.
§Visitor from ICREA/IFAE, Barcelona, Spain.

$^{\parallel}$Visitor from Centro de Investigacion en Computacion-IPN, Mexico City, Mexico.

¶Visitor from ECFM, Universidad Autonoma de Sinaloa, Culiacán, Mexico.

**Visitor from Universität Bern, Bern, Switzerland.

[1] J. Collins, D. Soper, and G. Sterman, Nucl. Phys. **B250**, 199 (1985).

[2] F. Landry, R. Brock, P. M. Nadolsky, and C. P. Yuan, Phys. Rev. D **67**, 073016 (2003).

[3] P. M. Nadolsky, D. R. Stump, and C. P. Yuan, Phys. Rev. D **64**, 114011 (2001).

[4] S. Berge, P. M. Nadolsky, F. Olness, and C. P. Yuan, Phys. Rev. D **72**, 033015 (2005). The parameters that control small-x broadening in RESBOS are set to the values given here.

[5] The boson rapidity is defined by $y = (1/2) \times \ln[(E + p_z)/(E - p_z)]$, where E is the energy and p_z is the momentum component parallel to the proton beam axis, and is given in terms of the momentum fractions, x_1 and x_2 of the incoming partons by $y = (1/2)\ln(x_1/x_2)$. Pseudorapidity is defined by $\eta = -\ln[\tan(\theta/2)]$, where θ is the polar angle.

[6] V. M. Abazov *et al.* (D0 Collaboration), Phys. Rev. Lett. **100**, 102002 (2008).

[7] V. M. Abazov *et al.* (D0 Collaboration), Phys. Lett. B **693**, 522 (2010).

[8] In the region $p_T^{\ell\ell} < 12$ GeV there were only five $p_T^{\ell\ell}$ bins in [6] and three $p_T^{\ell\ell}$ bins in [7].

[9] M. Vesterinen, T. R. Wyatt, Nucl. Instrum. Methods Phys. Res., Sect. A **602**, 432 (2009).

[10] A. Banfi, M. Dasgupta, and R. Delgado, J. High Energy Phys. 12 (2009) 022.

[11] A. Banfi, S. Redford, M. Vesterinen, P. Waller, and T. R. Wyatt, Eur. Phys. J. C **71**, 3 (2011).

[12] We follow the recommendations of J. M. Butterworth *et al.*, arXiv:1003.1643. The aim here is to avoid model dependencies in the correction factors by not correcting for the effects of final state bremsstrahlung or for events that fall outside the geometrical or kinematic acceptance of the experimental event selection.

[13] C. Balazs and C. P. Yuan, Phys. Rev. D **56**, 5558 (1997).

[14] P. B. Arnold and M. H. Reno, Nucl. Phys. **B319**, 37 (1989); **B330**, 284(E) (1990).

[15] P. Nadolsky *et al.*, Phys. Rev. D **78**, 013004 (2008).

[16] E. Barberio and Z. Was, Comput. Phys. Commun. **79**, 291 (1994).

[17] V. M. Abazov *et al.* (D0 Collaboration), Nucl. Instrum. Methods Phys. Res., Sect. A **565**, 463 (2006).

[18] T. Sjöstrand *et al.*, Comput. Phys. Commun. **135**, 238 (2001).

[19] R. Brun and F. Carminati, *CERN Program Library Long Writeup W5013*, 1993 (unpublished).

[20] M. L. Mangano *et al.*, J. High Energy Phys. 07 (2003) 001.

[21] See the supplemental material at http://link.aps.org/supplemental/10.1103/PhysRevLett.106.122001.